The Role of Fragility in Thermal Elastohydrodynamics

Scott Bair (scott.bair@me.gatech.edu)
Georgia Institute of Technology
Wassim Habchi
Lebanese American University

Research Article

Keywords: high-pressure rheology, viscosity, thermal elastohydrodynamic lubrication

Posted Date: October 5th, 2022

DOI: https://doi.org/10.21203/rs.3.rs-2116587/v1

The Role of Fragility in Thermal Elastohydrodynamics

Scott Bair*
Regents' Researcher, Retired
Georgia Institute of Technology, Center for High-Pressure Rheology
George W. Woodruff School of Mechanical Engineering, Atlanta, GA 30332-0405
email: scott.bair@me.gatech.edu
404-226-8012

Wassim Habchi
Department of Industrial and Mechanical Engineering, Lebanese American University
Byblos, Lebanon
wassim.habchi@lau.edu.lb

* Corresponding Author

Abstract

Temperature primarily influences thermal elastohydrodynamic lubrication (TEHL) through the temperature dependence of the viscosity of the liquid. The pressure and temperature dependences of viscosity increase rapidly as the glassy state is approached from the liquid state, a property known as fragility. The glass temperature increases with pressure and reaches to ordinary temperatures at TEHL pressures. It is astounding, therefore, that most TEHL analyses have ignored fragility by utilizing a viscosity correlation incapable of describing this behavior. Here, a low viscosity fragile oil is characterized for low-shear viscosity to 1.6 GPa and TEHL line contact simulations show, not only a substantial effect on friction, but significant differences in minimum film thickness when fragility is not ignored, as is customary in classical TEHL. The influence on friction manifests even under moderate load and speed conditions, while that on film thickness seems to be restricted to high loads.

Key Words: high-pressure rheology; viscosity; thermal elastohydrodynamic lubrication

1. Introduction

Readers of most research articles concerning thermal elastohydrodynamic lubrication (TEHL) may not be aware that the assumed response to temperature, pressure, and shear of the liquid lubricant is unlike that of any known oil. The property of fragility is ignored. The primary way in which temperature, T, affects the TEHL contact is the reduction in viscosity, μ, as quantified by a temperature-viscosity coefficient, $\beta = -\partial \ln \mu / \partial T$.

All lubricants are glass-forming, that is, they supercool (super-compress). Otherwise they would be solid at some ordinary conditions [1]. Glass-forming liquids experience a rapid increase in β as the glass transition is approached from the liquid state by cooling or compression. This effect is known as fragility [2]. Greater fragility implies that the short-range order is more rapidly destroyed by an increase in temperature, although the terminology is not dependent on the validity of this explanation. The glass transition temperature, T_g, increases with increasing pressure at the rate of 100 to 200 K/GPa. See for example reference [3]. When the glass transition is approached by compression from ambient pressure, as in TEHL, β may increase by an order-of-magnitude [4] from 0.03 to 0.3 K^{-1}. For accuracy and relevance, modelling of TEHL must include this behavior known as fragility.

The rapid increase in viscosity approaching the glass transition is not caused by the glass transition. Rather, the glass transition is caused by the slowing of the molecular dynamics by the large viscosity [5]. The response is slowed to the extent that the liquid can no longer relax to the equilibrium state on the experimental time scale and a solid-like response replaces the liquid-like response. This occurs at a characteristic viscosity, μ_g, independent of the pressure, making the glass transition, $T_g(p)$, an isoviscous state. Early work with molten minerals indicated that the glass transition viscosity was about $\mu_g \approx 10^{12}$ Pas. This value has often been used to define the glass transition [6]. However, measurements with organic liquids give a lower value of about $\mu_g \approx 10^{10}$ Pa·s [7,8]. Lubricating oils may have even lower values of μ_g [9]. Under ordinary circumstances, the wide range of values for μ_g would indicate a wide range of T_g; however, the rapid changes in viscosity with temperature and pressure near T_g means that the value is better characterized than might be expected.

The free volume theory of viscosity [10] has been useful for explaining and predicting the main features of the dependence of viscosity on temperature and pressure, though not always to experimental accuracy. The Doolittle [10] equation makes the low-shear viscosity a function of volume, V, and an occupied volume, V_{occ}.

$$\mu \propto \exp\left(B \frac{V_{occ}}{V - V_{occ}} \right) \qquad (1)$$

Obviously, the viscosity becomes unbounded as the volume is reduced to the occupied value by cooling or compression. The general shape of a plot of log viscosity versus pressure is explained by equation (1). The slower-than-exponential regime at low pressure results from the rapid decrease in compressibility with increasing pressure. The faster-than-exponential regime at high pressure results from the approach to the singularity at $V = V_{occ}$. Thus, the observed inflection and fragility is predicted by free volume theory [11].

In this article, the effect of ignoring fragility will be examined for one well-characterized oil.

2. The Temperature and Pressure dependence of the Viscosity of Dibutyl Phthalate

Viscosity reference liquids are extremely useful for the calibration of viscometers and for the validation of TEHL theory. One of these has been di(2-ethylhexyl) phthalate, DOS or DEHS [12]. Unfortunately, although this diester has been used extensively in TEHL, it has only been characterized to about 1 GPa pressure. Here, the viscosity of another phthalate diester will be accurately characterized to 1.6 GPa, to very near the glass pressure. There are three sources of high-pressure viscometer data for dibutyl phthalate, DBP. Irving and Barlow [13] performed measurements by falling cylinder up to 600 MPa at 30°C. Bair [11] used the same type of instrument up to 1250 MPa at 50°C. Cook et al. [14] employed the rolling ball technique in a diamond anvil cell to measure to 2900 MPa at 125°C. This is a very low viscosity oil of 9 cSt at 40°C.

In the diamond anvil, the ruby fluorescence pressure scale was employed for pressure measurement. This has been demonstrated to introduce error in pressure at low pressures [15]. These pressures are low considering the diamond anvil capability. Comparison with viscometer measurements indicate that the pressure is consistently 13% low at 50°C. Therefore, fragility is overstated in the diamond anvil viscometry and these data will not be used here.

Fortunately, another source of viscosity data comes from dielectric spectroscopy. Dufour and coworkers [16] found that for DBP the dielectric relaxation time is strongly correlated with viscosity along the ambient pressure isobar down to the glass transition. Casalini and Roland [17] at the Naval Research Laboratory, NRL, have measured the dielectric relaxation time, λ_D, at three temperatures and pressures to 1613 MPa. These data were converted to viscosity using $\mu/\lambda_D =$ 300 MPa.

2.1 The Improved Yasutomi Correlation

The Improved Yasutomi correlation utilizes the glass transition as an isoviscous state and describes the pressure dependence with

$$T_g(p) = T_{g0} + A_1 \ln(1 + A_2 p) \qquad (2)$$

Savin and coworkers [18] have determined that T_{g0} = -92.5°C for DBP by differential scanning calorimetry and this value is used in equation (2). Williams, Landel and Ferry [19] used a free volume form slightly different from the Doolittle equation (1) in that it specifies the thermal expansivity, F, of the free volume. Yasutomi made the relative thermal expansivity of the free volume fraction to be pressure dependent [11].

$$\mu = \mu_g \exp\left[\frac{-2.303 C_1 \left(T - T_g(p)\right) F(p)}{C_2 + \left(T - T_g(p)\right) F(p)}\right] \qquad (3)$$

Williams, Landel and Ferry had T_g and F being constant. The improved version employs a function for $F(p)$ which does not vanish at high pressure, thus avoiding the associated non-physical behavior.

$$F(p) = (1 + b_1 p)^{b_2} \qquad (4)$$

The improved Yasutomi correlation (2,3,4) was applied to the Bair [11] and NRL [17] data to arrive at the parameters listed in Table 1. The results of Irving and Barlow [13] were presented as a correlation and were not used although the agreement is good as shown in Figure 1.

Table 1. Parameters of the Improved Yasutomi correlation for DBP.

μ_g / Pa·s	9.36×10^{8}
A_1 / °C	195.6
A_2 / GPa^{-1}	0.533
b_1 / GPa^{-1}	15.73
b_2	-0.296
C_1	12.89
C_2 / °C	22.6

All the data are shown with the Improved Yasutomi correlation in Figure 1. Sekula et al.[20] have expressed the pressure dependence of the glass transition temperature by the Avramov equation. This is successfully compared with the present work in Figure 2 giving credibility to the accuracy of this correlation.

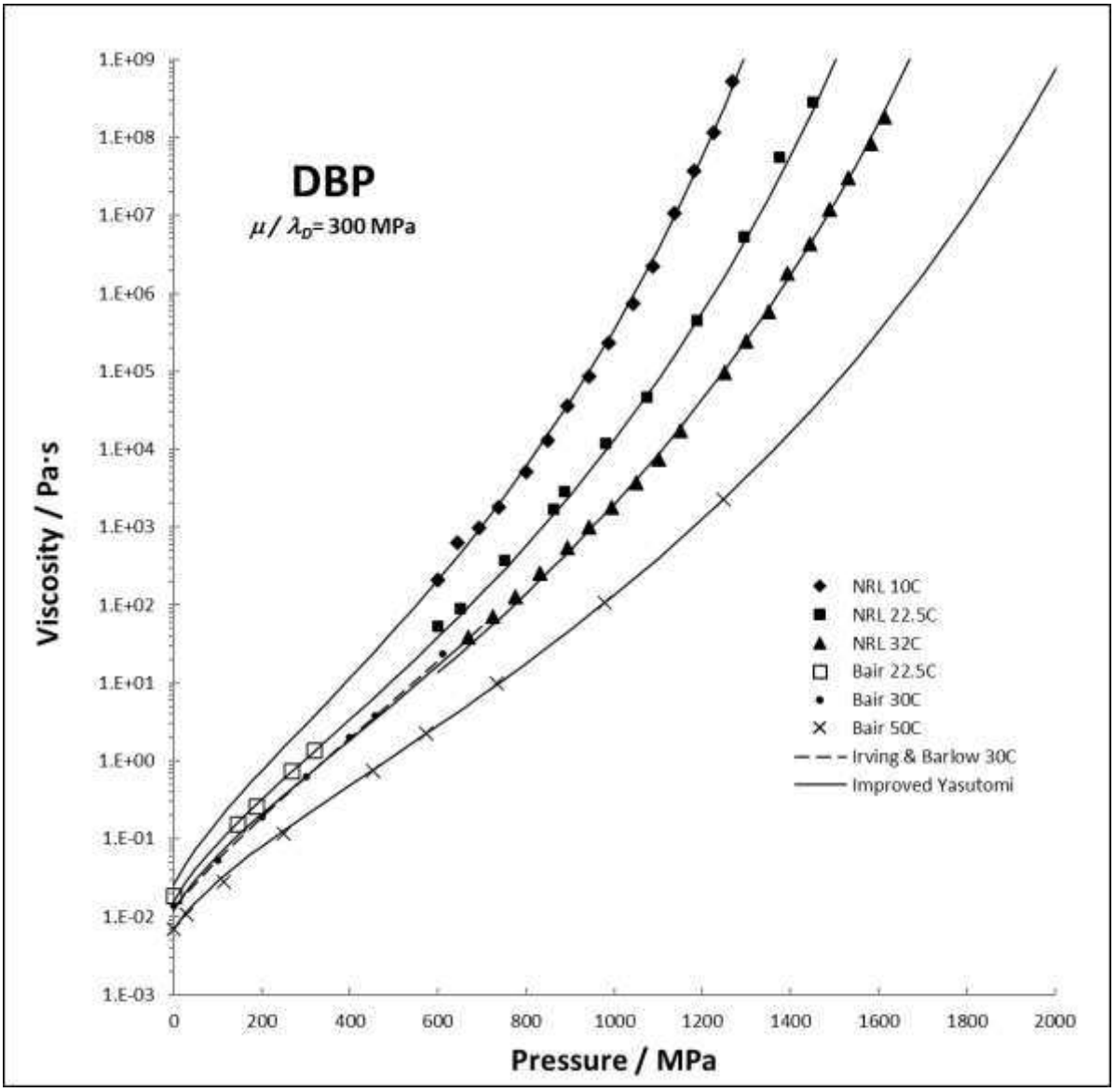

Figure 1. The viscosity of dibutyl phthalate has been measured by three laboratories at elevated pressures. The dielectric relaxation time has been reported to conditions approaching the glass transition. The improved Yasutomi correlation describes the data well. Reproduced from Bair, S. (2019). *High pressure rheology for quantitative elastohydrodynamics*. Elsevier by permission.

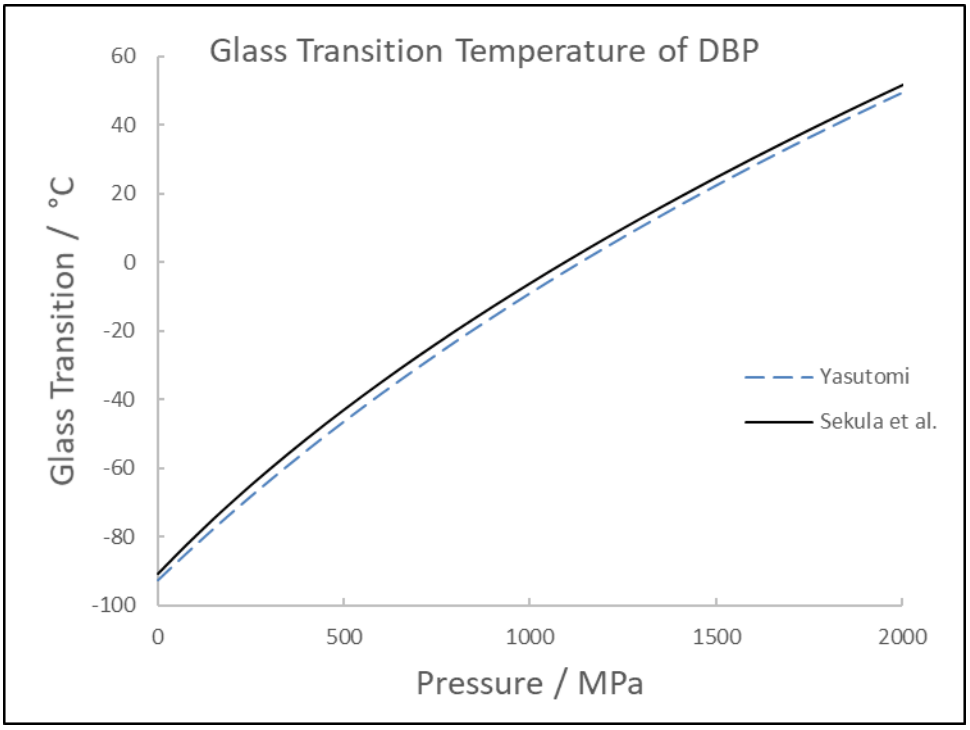

Figure 2. The pressure dependence of the glass transition temperature of DBP from reference [20] and from this work.

2.2 The Roelands Correlation

One of the surprising features of the classical field of TEHL has been the correlation most often chosen to represent the temperature and pressure dependence of viscosity, the Roelands equation [21].

$$\mu = \mu_p \left(\frac{\mu_R}{\mu_p} \right)^{\left[\left(\frac{p_P - p}{p_P} \right)^Z \left(\frac{T_R - T_\infty}{T - T_\infty} \right)^S \right]} \qquad (5)$$

The form used in TEHL has universal parameters given by $\mu_p = 6.31 \times 10^{-5}$ Pa·s , p_p = -0.196 GPa and $T_\infty = -135^{\circ}\mathrm{C}$. This application to TEHL is surprising because Roelands [21] invoked fragility (page 93) to impose an upper limit of 300 to 500 MPa (page 105) to the usefulness of this correlation, thus eliminating it as appropriate for TEHL analysis. For the typical case where $Z < 1$ the pressure dependence is always slower-than-exponential. Typically, for Roelands, the response is displayed as always curving downward in Figure 1, which can be seen to be correct only for $p < 300$ MPa. Inspection of equation (5) shows that the divergence temperature, sometimes

known as the ideal glass temperature, is always $T_\infty = -135^\circ\mathrm{C}$, irrespective of pressure. This is not physically acceptable.

The Roelands correlation (5) was applied to the viscometer measurements for $p \le 300\,\mathrm{MPa}$ assuming that the reference temperature is $T_R = 22.5°\mathrm{C}$. The fit to the data is shown in Figure 3 to be good with $\mu_R = 0.0186\,\mathrm{Pa{\cdot}s}$, $Z = 0.575$, and $S = 1.196$. Do not assume, from this successful application, that Roelands' correlation will always be accurate at low pressures. There are too few parameters. For low viscosity oils, Roelands cannot reproduce the rapid change in curvature of the logarithm of viscosity with pressure [22]. Roelands simply ignored such data in his plots [23].

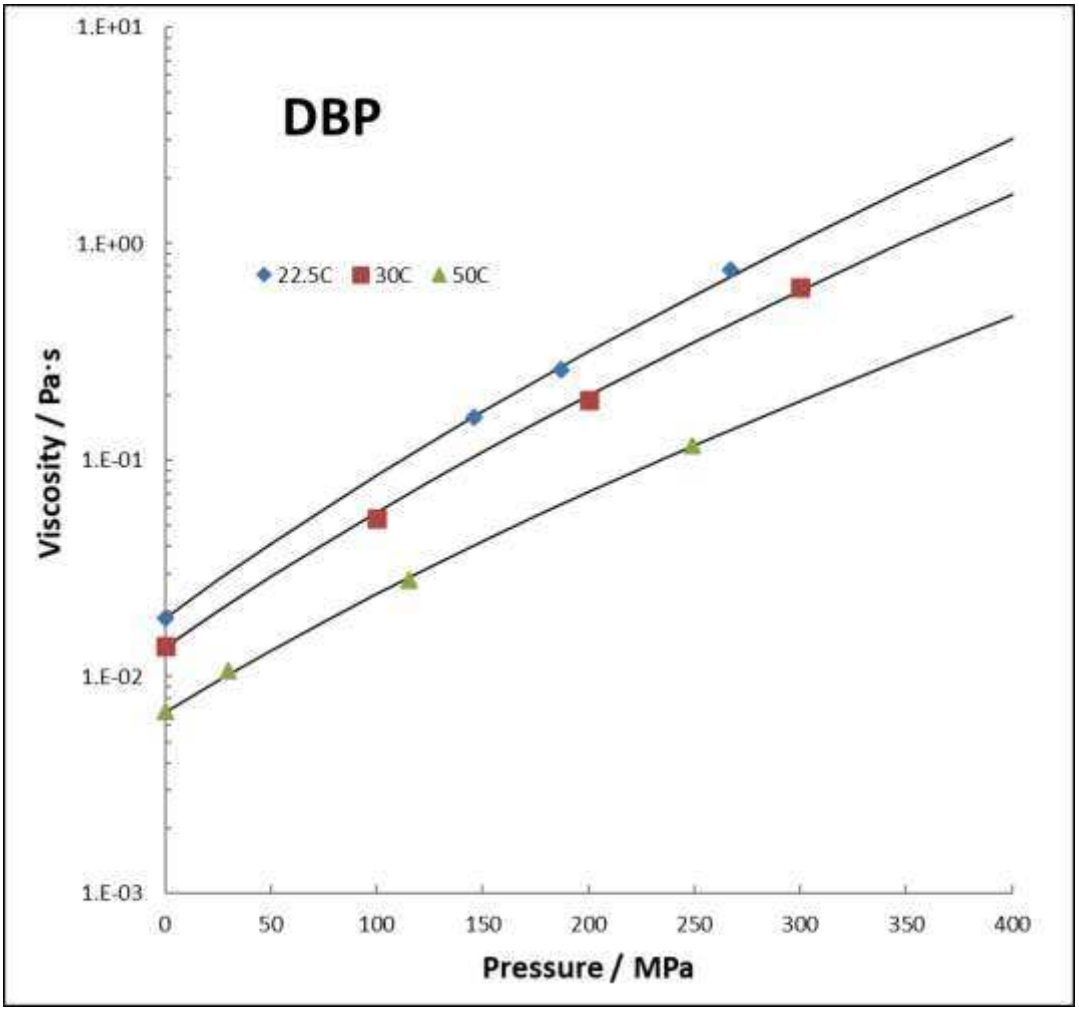

Figure 3. The viscosity of dibutyl phthalate fitted to the Roelands correlation at low pressures.

Figure 4 compares the real fragile pressure response of DBP, the Improved Yasutomi correlation, to the classical TEHL representation, extrapolated Roelands at 29°C. The real response to pressure was successfully described to 1.2 GPa by Bridgman [24] nearly a century ago. The pressure response that is being taught to tribology students in many textbooks, for example [25], is incorrect. The extrapolated Roelands curve in Figure 4 is not the response of any known liquid.

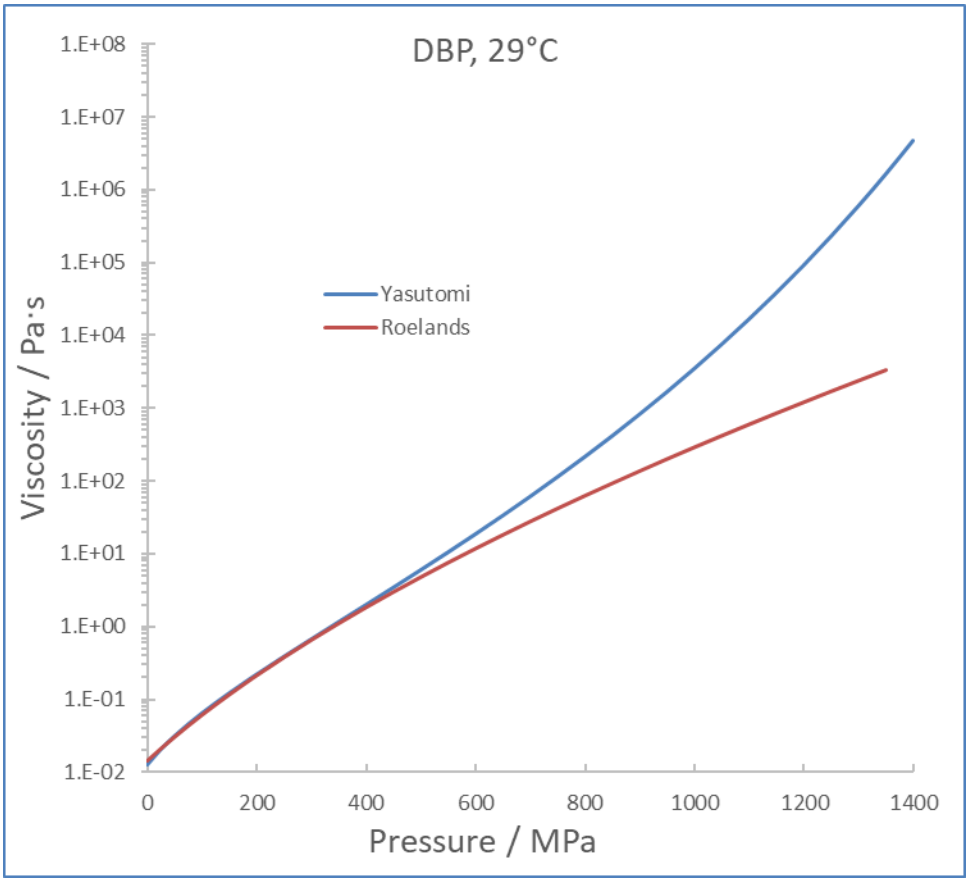

Figure 4. Comparing the real fragile pressure response, Improved Yasutomi, to the classical TEHL representation, extrapolated Roelands at 29°C.

2.3 The Temperature-Viscosity Coefficient of Dibutyl Phthalate

The temperature-viscosity coefficient defined by $\beta = -\partial \ln \mu / \partial T$ is plotted as a function of pressure at two temperatures, 20 and 50°C, in Figure 5. The classical approach using Roelands substantially understates the temperature dependence for pressures greater than about 500 MPa. To avoid having viscosity decrease with pressure at high temperature while maintaining the real temperature dependence, the faster-than-exponential pressure response is necessary [26]. The Roelands correlation in TEHL was strongly advocated by Houpert [27], who did not argue the

accuracy of the representation of viscosity but, rather, that this approach made the Eyring assumption appear to be accurate for traction.

It is likely that increased viscosity in Figure 4 and the increased temperature dependence in Figure 5, that is the fragility of DBP, will influence the friction and film thickness in TEHL.

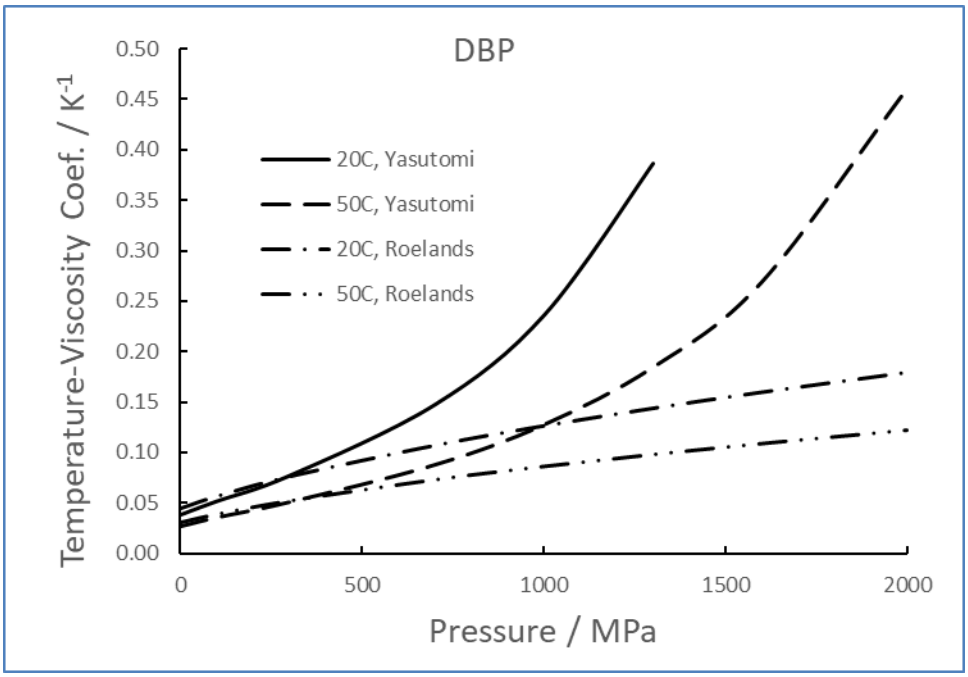

Figure 5. The temperature viscosity coefficient has been calculated from the Yasutomi correlation. The Roelands correlation extrapolated from data at pressures up to 300 MPa is compared.

4. TEHL Simulations

In order to inspect the influence of accurately modeling lubricant fragility on TEHL film thickness and friction predictions, some typical TEHL simulations are carried out here. Given that the focus is on rheological modeling, a line contact configuration is considered, out of simplicity. The full-system finite element framework is employed [28], using a full-coupling strategy as detailed in [29]. That is, all governing equations are solved simultaneously, guaranteeing a robust and fast resolution process. These equations are: the generalized Reynolds equation which governs the hydrodynamics of the lubricant flow, the linear elasticity equations which govern the elastic deformation of the contacting solids, the load balance equation which guarantees the equilibrium of forces over the contact, the energy equation which governs heat generation within the lubricating film and its transfer through the film and bounding solids, and finally the shear stress equation which governs the fluid shear stress distribution across the lubricating film.

The lubricant of choice is DBP. Its density-pressure-temperature dependence is modelled using the universal equation of state proposed by Bair [11], based on the Tait relation:

$$\frac{V}{V_0}=\frac{\rho_0}{\rho}=1-\frac{1}{1+K_0'}\ln\left[1+\frac{p}{K_0}\left(1+K_0'\right)\right] \qquad (6)$$

With $K_0=K_{00}\exp\left(-\beta_K T\right)$ and $V_0/V_R=\rho_R/\rho_0=1+a_V\left(T-T_R\right)$. The following values are adopted for the Tait parameters: $K_0'=11$, $a_V=8\times10^{-4}\mathrm{K}^{-1}$, $K_{00}=9\mathrm{GPa}$, and $\beta_K=6.5\times10^{-3}\mathrm{K}^{-1}$. The reference state temperature, $T_R=300\mathrm{K}$, which yields a reference state density, $\rho_R=994\,\mathrm{kg/m}^3$. Then the density-pressure-temperature relation is obtained by multiplying ρ_R/ρ_0 by ρ_0/ρ. The shear-dependence of DBP is represented by the modified Carreau equation, which relates the generalized-Newtonian viscosity η to the low-shear Newtonian one μ, the shear stress τ, and the shear modulus G as follows:

$$\frac{\eta}{\mu}=\left[1+\left(\frac{\tau}{G}\right)^2\right]^{\frac{1-\frac{1}{n}}{2}} \qquad (7)$$

The values of the Modified Carreau parameters were estimated from data [11] on DEHP to be $n=0.41$ and $G=8.4\mathrm{MPa}$. The limiting shear stress τ_L is assumed to vary linearly with pressure according to $\tau_L=\Lambda p$, with $\Lambda=0.04$. That is, lubricant shear stress τ is truncated to τ_L whenever it exceeds the latter. Finally, for the viscosity-pressure-temperature dependence of DBP, the two responses detailed earlier are considered (i.e. the real one / Yasutomi and the classical one / Roelands) to isolate the effect of fragility, all other properties being unchanged.

The thermal conductivity of DBP is taken to be $k=0.134\,\mathrm{W/m.K}$ and its heat capacity $c=2590\,\mathrm{J/kg.K}$. The inlet temperature is taken to be: $T_0=29^{\circ}\mathrm{C}$. Steel-Steel smooth line contacts operating under steady-state regime are considered. That is, the contact is subject to a constant external applied load, *F* (per unit length), and a constant mean entrainment speed, $u_m=\left(u_1+u_2\right)/2$. The individual velocities u_1 and u_2 of the solid surfaces are varied such that the mean entrainment speed is kept constant, while the slide-to-roll ratio $\sum=\left(u_2-u_1\right)/u_m$ is varied from 0 to 1. A roller radius $R=15mm$ is adopted. Two different values are considered for the external applied load; a moderate and a high load with $F=0.2MN/m$ and $F=1MN/m$, respectively. The corresponding Hertzian contact pressures are $p_h=0.7\mathrm{GPa}$ and $p_h=1.56\mathrm{GPa}$, respectively. The glass temperature at the highest pressure is 26°C. Two values are also considered for the mean entrainment speed; a moderate and a high speed with $u_m=0.5\,\mathrm{m/s}$ and $u_m=3\,\mathrm{m/s}$, respectively. The results of the TEHL simulations are reported in figures 6 and 7, for the considered moderate and high-speed cases, respectively. Each figure shows for both responses (Yasutomi and Roelands) the friction curves (top), film thickness curves (middle), and maximum temperature rise $\Delta T_{\max}$

within the lubricating film (bottom) which is usually located at the contact center, against the slide-to-roll ratio $\sum$, for both the moderate (left) and high (right) load cases considered. The friction curves show variations of the friction coefficient f with $\sum$, where the former corresponds to the ratio of the shear force (evaluated over the mid-layer of the lubricating film) to the external applied load F. Note that isothermal friction curves are also reported in dashed lines. As for film thickness curves, they show variations of central film thickness h_c and minimum film thickness h_m with $\sum$, with isothermal curves being also reported in dashed lines. The effect of roller elastic creep has been ignored.

First, in terms of friction, it is clear that frictional response is significantly affected by fragility, even under moderate load and speed conditions. Even under isothermal conditions, the frictional responses of Roelands and Yasutomi are different. This is because friction is governed by the viscous behavior of the lubricant in the central part of the contact domain (i.e., the high-pressure region). But, under high pressure, the two viscosity-pressure responses exhibit significant deviations (see Figure 4). Therefore, the isothermal friction curves reveal the influence of pressure fragility on friction (though it is smeared by the limiting shear stress for high F and $\sum$), whereas the thermal curves reveal the combined effects of both temperature and pressure fragility.

As for film thickness, the influence of fragility seems to be limited to high loads. For the considered moderate load, only under high speed and high slide-to-roll ratio is any difference between the Roelands and Yasutomi responses noticeable. Also note that isothermal film thickness curves perfectly overlap. This is because film thickness is governed by viscous behavior in the inlet part of the contact (i.e. the low-pressure region). But, under low pressure (up to 300MPa), at the considered inlet temperature of 29^{o}C, the two viscosity-pressure responses overlap (see figure 4). This means that the reported differences in film thickness responses under high load conditions are purely related to temperature fragility, and the relatively high temperature rise within the lubricant film under these conditions (see bottom right sub-figures in figures 6 and 7). It is safe to say that the influence of temperature fragility increases with both load and speed; as does the temperature rise within the lubricating film. Finally, note that for the high-speed case, even under pure-rolling conditions, thermal film thickness curves deviate from isothermal ones, indicating substantial inlet heating by compression [30] due to increased inlet pressures, as the mean entrainment speed is increased.

5. Conclusion

An accurate correlation of the temperature and pressure dependences of the low-shear viscosity of a diester oil at pressures to 1.6 GPa has been developed from experimental measurements of viscosity and dielectric spectroscopy. These data have been fitted to the Improved Yasutomi correlation which employs the glass transition as an isoviscous state. The accuracy of the pressure dependence of the glass transition temperature thus obtained has been verified. This is clearly a fragile liquid. The correlation preferred in classical TEHL, the Roelands

equation, cannot describe pressure fragility. TEHL line contact simulations show, not only a substantial effect on friction, but significant differences in minimum film thickness when fragility is not ignored, as is customary in classical TEHL. The influence on friction manifests even under moderate load and speed conditions, while that on film thickness seems to be restricted to high loads.

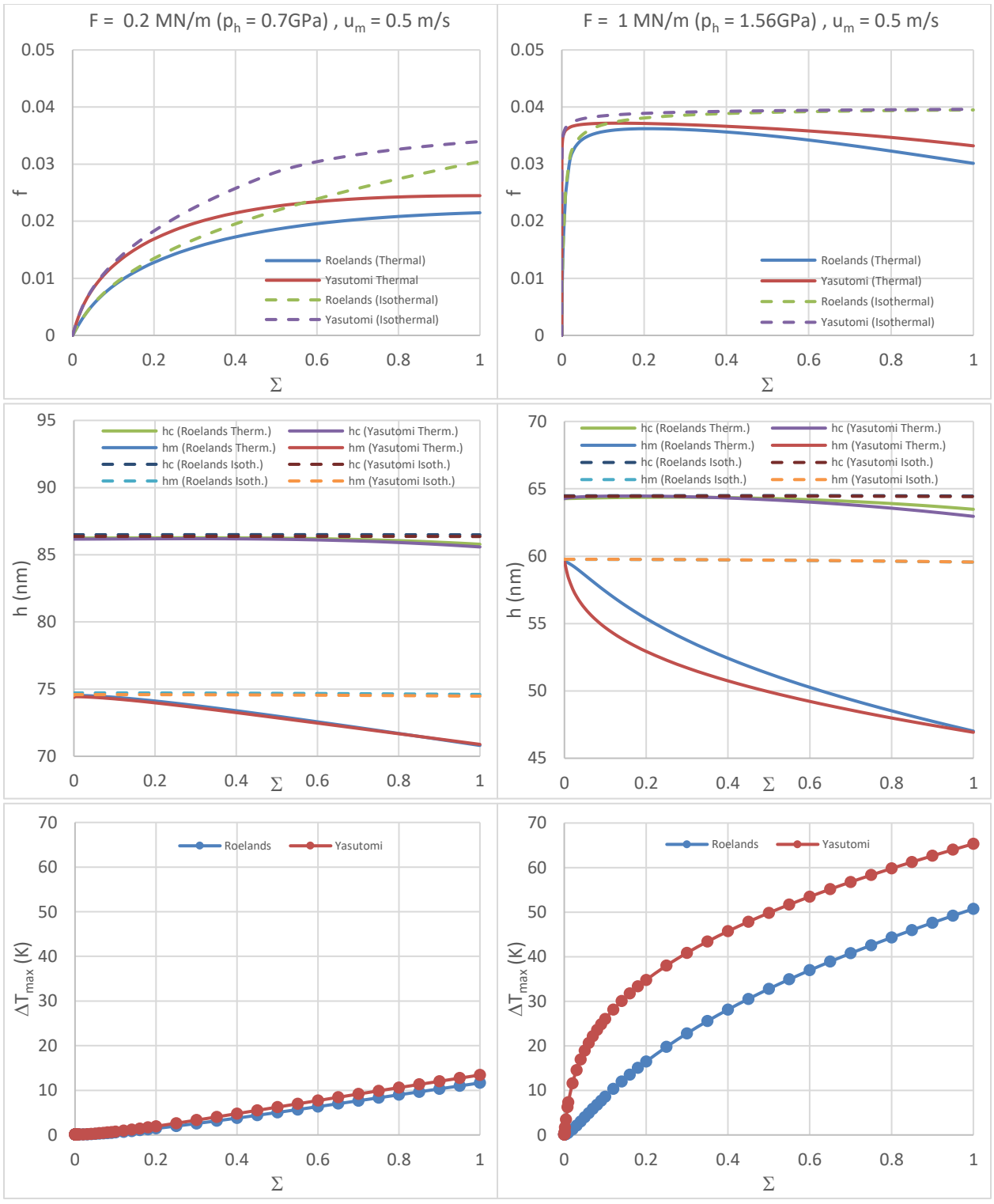

Figure 6. Influence of lubricant temperature fragility on friction (top), film thickness (middle) and maximum temperature rise within the lubricating film (bottom), for the moderate (left) and high (right) load cases, under moderate mean entrainment speed conditions (u_m = 0.5m/s).

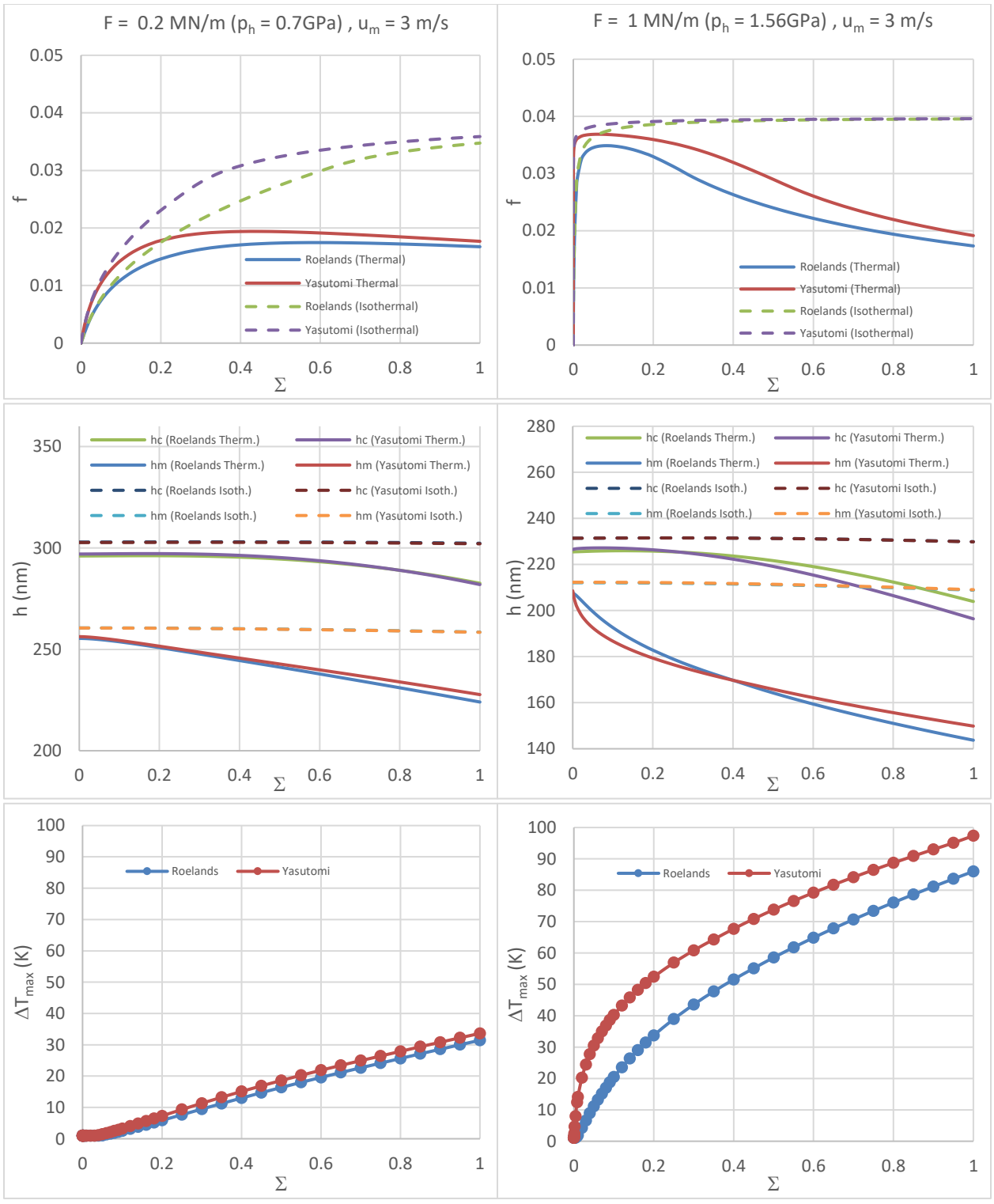

Figure 7. Influence of lubricant temperature fragility on friction (top), film thickness (middle) and maximum temperature rise within the lubricating film (bottom), for the moderate (left) and high (right) load cases, under high mean entrainment speed conditions (u_m = 3 m/s).

References

[1] Harrison, G. (1976). The dynamic properties of supercooled liquids. *London and New York*.

[2] Angell, C. A. (1991). Relaxation in liquids, polymers and plastic crystals—strong/fragile patterns and problems. *Journal of Non-Crystalline Solids*, *131*, 13-31.

[3] Paluch, M., Hensel-Bielowka, S., & Zioło, J. (1999). Effect of pressure on fragility and glass transition temperature in fragile glass-former. *The Journal of chemical physics*, *110*(22), 10978-10981.

[4] Bair, S. (2020). Viscous heating in compressed liquid films. *Tribology Letters*, *68*(1), 1-12.

[5] Leutheusser, E. (1984). Dynamical model of the liquid-glass transition. *Physical Review A*, *29*(5), 2765.

[6] Mauro, J. C., Yue, Y., Ellison, A. J., Gupta, P. K., & Allan, D. C. (2009). Viscosity of glass-forming liquids. *Proceedings of the National Academy of Sciences*, *106*(47), 19780-19784.

[7] Schröter, K., & Donth, E. (2000). Viscosity and shear response at the dynamic glass transition of glycerol. *The Journal of Chemical Physics*, *113*(20), 9101-9108.

[8] Plazek, D. J., & Magill, J. H. (1966). Physical properties of aromatic hydrocarbons. I. Viscous and viscoelastic behavior of 1: 3: 5-Tri-α-naphthyl benzene. *The Journal of chemical physics*, *45*(8), 3038-3050.

[9] Bair, S. (2019). The viscosity at the glass transition of a liquid lubricant. *Friction*, *7*(1), 86-91.

[10] Turnbull, D., & Cohen, M. H. (1970). On the free-volume model of the liquid-glass transition. *The journal of chemical physics*, *52*(6), 3038-3041.

[11] Bair, S. S. (2019). *High pressure rheology for quantitative elastohydrodynamics*. Elsevier.

[12] Harris, K. R. (2009). Temperature and pressure dependence of the viscosities of 2-ethylhexyl benzoate, bis (2-ethylhexyl) phthalate, 2, 6, 10, 15, 19, 23-hexamethyltetracosane (squalane), and diisodecyl phthalate. *Journal of Chemical & Engineering Data*, *54*(9), 2729-2738

[13] Irving, J. B., & Barlow, A. J. (1971). An automatic high pressure viscometer. *Journal of Physics E: Scientific Instruments*, *4*(3), 232.

[14] Cook, R. L., King Jr, H. E., Herbst, C. A., & Herschbach, D. R. (1994). Pressure and temperature dependent viscosity of two glass forming liquids: glycerol and dibutyl phthalate. *The Journal of chemical physics*, *100*(7), 5178-5189.

[15] Casalini, R., Bair, S. S., & Roland, C. M. (2016). Density scaling and decoupling in o-terphenyl, salol, and dibutyphthalate. *The Journal of Chemical Physics*, *145*(6), 064502.

[16] Dufour, J., Jorat, L., Bondeau, A., Siblini, A., & Noyel, G. (1994). Shear viscosity and dielectric relaxanon time of dibutyl phthalate down to glass transition temperature. *Journal of Molecular Liquids*, *62*(1-3), 75-82.

[17] Casalini, R., & Roland, C. M. (2007). Isobaric and isochoric properties of glass-formers. In *Soft Matter under Exogenic Impacts* NATO Science Series II, 242 (pp. 141-147). Springer, Dordrecht.

[18] Savin, D. A., Larson, A. M., & Lodge, T. P. (2004). Effect of composition on the width of the calorimetric glass transition in polymer–solvent and solvent–solvent mixtures. *Journal of Polymer Science Part B: Polymer Physics*, *42*(7), 1155-1163.

[19] Williams, M. L., Landel, R. F., & Ferry, J. D. (1955). The temperature dependence of relaxation mechanisms in amorphous polymers and other glass-forming liquids. *Journal of the American Chemical society*, *77*(14), 3701-3707.

[20] Sekula, M., Pawlus, S., Hensel-Bielowka, S., Ziolo, J., Paluch, M., & Roland, C. M. (2004). Structural and secondary relaxations in supercooled di-n-butyl phthalate and diisobutyl phthalate at elevated pressure. *The Journal of Physical Chemistry B*, *108*(16), 4997-5003.

[21] Roelands, C.J.A. 1966, Correlational Aspects of the Viscosity-Temperature-Pressure Relationship of Lubricating Oils. Ph.D. Thesis, Technical University Delft, Delft, The Netherlands, Groningen, The Netherlands, 1966.

[22] Bair, S. (2016). Pressure–viscosity response in the inlet zone for quantitative elastohydrodynamics. *Tribology International*, *97*, 272-277.

[23] Bair, S. (2004). Roelands' missing data. *Proceedings of the Institution of Mechanical Engineers, Part J: Journal of Engineering Tribology*, *218*(1), 57-60.

[24] Bridgman, P. W. (1925). The viscosity of liquids under pressure. *Proceedings of the national academy of sciences*, *11*(10), 603-606.

[25] Gohar, R., & Rahnejat, H. (2012). *Fundamentals of tribology, 2nd Ed*. World Scientific Publishing Company, Hackensack, NJ, p. 90.

[26] Bair, S. (2012). A critical assessment of the role of viscometers in quantitative elastohydrodynamics. *Tribology transactions*, *55*(3), 394-399.

[27] Houpert, L. (1985). New results of traction force calculations in elastohydrodynamic contacts. *ASME J Tribology, 107*, 241-245.

[28] Habchi W. - Finite Element Modeling of Elastohydrodynamic Lubrication Problems, 2018, *Wiley*, Chichester, UK, ISBN: 978-1-119-22512-6.

[29] Habchi W. - Coupling Strategies for Finite Element Modeling of Thermal Elastohydrodynamic Lubrication Problems, *ASME J Tribology*, 2017, vol. 139 (4), 041501.

[30] Habchi W. and Vergne P. - On the Compressive Heating/Cooling Mechanism in Thermal Elastohydrodynamic Lubricated Contacts, *Tribology International*, 2015, vol. 88, pp. 143-152.